REMARKS

Applicants hereby confirm that the invention of Group I including Claims 1, 2, 4-12, 14-19 and 21-33 has been elected. The remaining Claims 34-40 and 43-44 have been cancelled.

Claim 33 is rejected under 35 U.S.C. 112, paragraph 1, as based on a disclosure which is not enabling. Specifically, the Examiner rejected Claim 33 on the grounds that it is not clear "why one would drill PC holes through the active layer or leave the holes above the active layer is not included in the Specification." The rejection of Claim 33 under 35 U.S.C. 112, paragraph 1, is respectfully traversed. It is believed that 35 U.S.C. 112, paragraph 1 does not impose any requirement that reasons be given for any particular claimed feature. If the Examiner disagrees, it is respectfully requested that the Examiner provide the proper legal basis for such a requirement.

The Examiner also rejected Claim 33 under 35 U.S.C. 112, paragraph 1, on the grounds that "there was no mention of a plurality of active layers in the Specification which is implied by the phrase 'to a region between the substrate and the active layers.'" Claim 33 has now been amended so that only one active layer is recited. Therefore, there is no implication that a plurality of active layers is present in Claim 33.

Claim 33 is rejected under 35 U.S.C. 112, paragraph 2, as being indefinite. In particular, Claim 33 is rejected on the grounds that the term "band gap" is ambiguous as to whether this term refers to the electronic or photonic band gap. Claim 33 has been amended to clarify that this term refers to the electronic band gap.

Based on the above, Claim 33 is believed to be in compliance with 35 U.S.C. 112.

The Drawings are objected to on the grounds that the band structure diagrams of the active layer and of the substrate are not shown. Attached is Fig. 8 illustrating the energy band gap of a material. The specification has also been amended to refer to or describe Fig. 8. No new matter is believed to have been introduced by the new figure, and the description thereof added to the description.

Claims 1, 2, 4, 5, 7-12, 14-19, and 21-33 are rejected under 35 U.S.C. 102(e) as being anticipated by U.S. Patent No. 6,958,494 to Lin et al. The rejection is respectfully traversed.

The device of claim 1 and that of claim 33 includes at least one waveguide layer adjacent to the active layer, where the at least one waveguide layer and the active layer trap the light generated by the active layer. There is no waveguide layer in Lin, and for this reason, there is no

identity of elements between Lin et al. on one hand and Claims 1 and 33 on the other. It is believed to be well settled that in order for a reference to anticipate a claim, there must be identity of elements between those of the reference and those of the claim. Since Lin fails to disclose at least one waveguide layer adjacent to the active layer where the at least one waveguide layer and the active layer trap the light generated by the active layer, the Lin patent does not anticipate Claims 1 and 33. Since Lin fails to anticipate Claims 1 and 33, it likewise fails to anticipate Claims 2, 4, 5, 7-12, 14-19 and 21-32 dependent upon Claim 1.

Claim 33 is rejected under 35 U.S.C. 102(b) as being anticipated by U.S. Patent No. 5,955,749 to Joannopoulos. The rejection is respectfully traversed as applied to Claim 33 as amended.

Claim 33 has been amended to include at least one waveguide layer adjacent to the active layer, where the at least one waveguide layer and the active layer trap the light generated by the active layer. Joannopoulos fails to teach or suggest at least one waveguide layer adjacent to the active layer where the at least one waveguide layer and the active layer trap the light generated by the active layer. Hence, there is no identity of elements between Joannopoulos and Claim 33 so that the anticipation rejection fails.

As explained in Paragraph [0003] of the present Application, the light extraction efficiency is one of the main themes for improving the energy efficiency of light-emitting devices. Since waveguides are used for confining light, there appears to be no reason or motivation for one skilled in the art to modify the light-emitting device of Joannopoulos to include a waveguide layer. Claim 33 is therefore believed to be non-obvious over Joannopoulos. For the same reason, the rejected claims 1, 2, 4, 5, 7-12, 14-19, and 21-33 are also believed to be non-obvious over U.S. Patent No. 6,958,494 to Lin et al.

Claims 1, 2, 4, 5, 14-17, 28, 29, 31, 32 are rejected under 35 U.S.C. 103(a) as being unpatentable over the Erchak et al. article entitled "Enhanced coupling to vertical radiation using a two-dimensional photonic crystal in a semiconductor light-emitting diode," Applied Physics Letters, Volume 78, No. 5, January 29, 2001, Page 563-565, in view of U.S. Patent Application No. 2001/0038656 to Takeuchi et al. The rejection is respectfully traversed.

The Examiner is of the opinion that Erchak discloses all of the limitations of Claim 1 except that it fails to disclose the waveguide layers, their band gap and the positional relationships. The Examiner is also of the opinion that Takeuchi teaches a first structure

comprising at least one waveguide layer adjacent to the active layer referencing Paragraphs [0025] and [0027] of Takeuchi. The Examiner is then of the opinion that "it would have been obvious to one skilled in the art (e.g. an optical engineer) at the time the invention was made, to add the extra layers of Takeuchi to the device of Erchak in the manner claimed, for the advantage of even greater light confining capacity (see Paragraphs [0002-0004] of Takeuchi." See Page 9 of the Office Action. We disagree.

As noted above, the common and widely recognized problems encountered in light-emitting devices is the problem of increasing the amount of light that can be extracted from the light-emitting devices. This problem is explained, for example, in Chapter 5 of the book "Introduction to Solid-State Lighting" by Arturas Zukauskas et al., 2002, ISBN 0-471-21574-0, of which pages 82-91 and 112-115 are attached. As mentioned on page 83 of this book, "the main physical reason that light extraction is difficult is the large ratio of the refractive indices of the semiconductor and the surrounding media. Consequently, a major part of the light generated inside a chip is reflected back into the semiconductor." Since the reflection of the light generated inside a chip back into the semiconductor is the major problem encountered in light emitting devices, there is therefore no reason or motivation for one skilled in the art to employ a device such as a waveguide that will confine light to, instead of extract light from, the light-emitting devices.

The laser device of Takeuchi operates on an entirely different principle from the light-emitting device of Erchak or of the present rejected claims. In a laser device such as in Takeuchi, light must be confined within a cavity so that the photons within the cavity would further stimulate light emission in the active layer of the laser. The cavity is typically confined by means of reflective layers on both sides of the cavity facing each other. In Takeuchi, for example, this is accomplished by the layers below and above the active layer: the optical confinement layers 25 and 27 and the cladding layers 24 and 28. As in a typical laser diode, since these layers are not perfect reflectors, a typically small portion of the light will pass and escape through these layers to provide laser light. Since the radiation generated by lasers originate from stimulated emission, the light emitted has high intensity and one skilled in the art typically will not be concerned with the problem of light extraction. Thus, even though the leakage through the reflective layers of the cavity may be small, such leakage will provide adequate output due to the fact that the stimulated emission generates light of high intensity so

that leakage of a small portion of the light generated is adequate for various laser applications. The situation is entirely different with light emitting devices, where there is no stimulated emission or lasing function and light extraction becomes a major problem. Furthermore, the light emitted by light-emitting devices is typically incoherent versus coherent light emitted by lasers.

Since the major concern for light emitting devices is the ability to extract sufficient light, adding a light confining structure will not address this problem, and may worsen the problem. Because of the above differences, there is simply no reason or motivation for one skilled in the art to look to structures that confine light in lasers for application to light emitting devices.

The reason given by the Examiner above for combining Takeuchi with Erchak is "for the advantage of even greater light confinement capacity (see [0002-0004] of Takeuchi)." Page 9 of the Office Action. The Examiner's reliance on such advantage in Takeuchi is misplaced. This advantage described in Takeuchi is exactly the wrong solution for solving the problem of inadequate light extraction for light-emitting devices. Therefore, we believe that the reason supplied by the Examiner for combining Takeuchi with Erchak will not motivate one with ordinary skill in the art to perform the combination urged by the Examiner.

Furthermore, the waveguide layers (nitride semiconductor device) described in Paragraphs 25 and 27 of Takeuchi are crystalline layers. The Bragg reflector (DBR) of Erchak, composed of aluminum oxide and gallium arsenide, is not crystalline. It is therefore not clear how the crystalline waveguide structures of Takeuchi may be formed adjacent to and in contact with the non-crystalline structure in Erchak to make a practical device. The Examiner has failed to explain how this can be done.

Claim 1 further contains the limitation that an index of refraction of said at least one waveguide layer is higher than that of the cladding layers. This further distinguishes from Erchak

Based on the above, it is believed that there is no reason or motivation for combining Takeuchi with Erchak in the manner urged by the Examiner and that furthermore it is not clear how the two may be combined in view of their very different structures as noted above. Hence, Claims 1 and 33 are believed to be non-obvious over Erchak and Takeuchi. Claims 1 and 33 are therefore believed to be allowable.

The reason for employing at least one waveguide in the light emitting device of claims 1 and 33 is as follows. As clearly explained in paragraph [0017] of the present application, in one embodiment, the waveguide layers 122 and 123 have the important function of trapping optical power along the waveguide in one single mode or a few lower-order modes. By confining the optical power to a single mode or a few lower-order modes, this renders the extraction by photonic crystal of the light emitted by the active layer particularly effective. As noted in paragraph [0017], "extraction by Photonic Crystal would not be effective if the waveguide supports a number of modes with quite different propagation constants because the band edge of PC structure may correspond to only one mode or a few modes." Such rationale is not taught or suggested by Erchak and Takeuchi.

In Claim 2, the Examiner is of the opinion that the DBR structure (first structure) in Erchak contains substantially a single optical mode (935 nm in one embodiment and at 790 nm in another, referencing first column of page 565, second and third paragraphs, respectively). We respectfully disagree. First, the wavelength that is extracted from the first structure is different from the optical modes that may be present in the first structure. Thus, each of the 935 nanometer components and the 790 nanometer components that are extracted may have many different modes so that the fact that a single wavelength component may be extracted does not mean that only a single mode or a few lower order modes are extracted. In other words, wavelength of the light should not be confused with the optical modes. Second, what is extracted by the photonic crystal is only a part of the optical power present in the first structure. Hence the characteristics of the optical power extracted by the photonic crystal itself do not necessarily indicate what optical modes may be present in the first structure. If the Examiner disagrees, it is respectfully requested that the Examiner explain in detail and with factual support why in his view the DBR and the active layer in Erchak contain only a single optical mode. This was pointed out in the amendment mailed on May 19, 2006 in response to an earlier Office Action. The present Office Action failed to respond to the distinctions above. If the rejection of claim 2 is maintained in the next Office Action, it is respectfully requested that these distinctions be addressed specifically.

Before the rejection of claim 4 is discussed, it will be useful to first examine the nature of the DBR structure of Erchak. We believe that the DBR structure of Erchak cannot be a waveguide layer. A Bragg reflector is typically made of alternating layers of high index of

refraction materials and low index of refraction materials. Thus the DBR structure merely reflects light that is incident upon it in a normal or near normal direction, but absorbs or transmits light that is incident on the structure at angles tens of degrees away from the normal direction. For this reason, the DBR structure fails to trap light and is not suitable for a waveguide. References for the Examiner (Wikipedia definition of DBR and article from the world wide web on optical waveguides) were submitted with the May 19, 2006 amendment. As clearly explained in these references, an optical waveguide guides light by total internal reflection and typically includes a core and cladding surrounding the core, where the claddings are made of a material with a slightly lower index of refraction than the core. This difference in the indices causes total internal reflection to occur at a cladding/core interface. The DBR structure of Erchak regarded by the Examiner as the waveguide clearly fails to match either the structure or function of the optical waveguides described in the reference on optical waveguides attached to the May 19, 2006 amendment.

On claim 4, since the DBR layers of Erchak cannot be the waveguide layer, whatever may be the thickness of the layers of the DBR is irrelevant in regard to the thickness of the at least one waveguide layer of claim 4. This was pointed out in the amendment mailed on May 19, 2006 in response to an earlier Office Action. The present Office Action failed to respond to the distinctions above. If the rejection of claim 4 is maintained in the next Office Action, it is respectfully requested that this distinction be addressed specifically.

On claim 5, the Examiner is of the opinion that the device by Erchak comprises a transparent and conductive layer (AlxOy layer) over the first structure (second paragraph of first column of page 563). We disagree. The Al_xO_y layer in Erchak is located below the active layer and is therefore not over the first structure which comprises the at least one waveguide layer, the active layer and two cladding layers. Furthermore, the AlxOy layer in Erchak is not electrically conductive.

In addition to the above, claims 2, 4, 5, 12, 14-17, 28-32 are further believed to be allowable since they depend from allowable claim 1.

Claims 7-11 are rejected under 35 U.S.C. 103(a) as being unpatentable over Erchak and Takeuchi and further in view of common knowledge in the art. Claims 18, 19 and 21 are rejected under 35 U.S.C. 103(a) as being unpatentable over Erchak and Takeuchi and further in view of USP 6,420,732 to Kung. Claims 22-26 and 43-44 are rejected under 35 U.S.C. 103(a) as

being unpatentable over Erchak and Takeuchi and further in view of WO 01/91194 to Baur. Claims 43-44 have been cancelled. Claim 27 is rejected under 35 U.S.C. 103(a) as being unpatentable over Erchak in view of Kung. The rejections are respectfully traversed. None of the supplementary references (common knowledge, Kung, Baur) remedies the deficiencies of the primary references, Erchak and Takeuchi. Hence independent claims 1 and 33 are patentable over all of the above references, and claims 7-11, 18, 19, 21-27 are believed to be patentable as well.

CONCLUSION

In view of the amendments and remarks contained herein, it is believed that all pending claims 1, 2, 4, 5, 7-12, 14-19 and 21-33 are in condition for allowance and an indication of their allowance is requested. However, if the Examiner is aware of any additional matters that should be discussed, a call to the undersigned attorney at: (415) 318-1162 would be appreciated.

Respectfully submitted,

James S. Hsue
Reg. No. 29,545

October 18, 2006
Date

PARSONS HSUE & de RUNTZ LLP
595 Market Street, Suite 1900
San Francisco, California 94105
Telephone: 415.318.1160 (main)
Telephone. 415.318.1162 (direct)
Fax: 415.693.0194

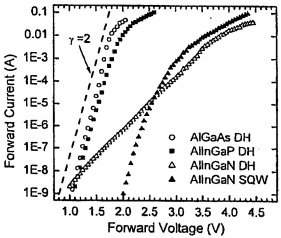

FIG. 4.3.10. Current–voltage characteristics of AlGaAs-, AlGaInP-, and AlInGaN-based high-brightness LEDs.

Temperature characteristics of high-brightness LEDs are discussed by Steranka (1997) and Mukai *et al.* (1998c, 1999). Generally, all LEDs exhibit a red shift of the peak wavelength with increasing temperature because of the temperature-induced bandgap shrinkage. As a rule, the output power decreases with operating temperature, since the radiative recombination rate decreases and the nonradiative recombination rate increases. However, the decrease in output power is more characteristic of AlGaAs and AlGaInP LEDs than of nitride-based LEDs. This is caused by the absence of the close indirect valleys in the band structure of AlInGaN-based semiconductors, in contrast to arsenide- and phosphide-based materials.

CHAPTER 5

Introduction to Solid-State Light
by Artūras Žukauskas, 2002
ISBN 0-471-21574-0

LIGHT EXTRACTION FROM LEDs

For many years, most of the LEDs manufactured employed a primitive design that featured a planar structure on an absorbing substrate encapsulated in an epoxy dome. Such design resulted in extremely poor light-extraction efficiency ($\eta_{opt} \approx 4\%$), much less than typical internal quantum efficiencies. Since the external quantum efficiency of such LEDs was just a few percent, they were able to compete with other light sources only for applications in color indicator lamps and miniature numeric displays, where small dimensions and extended lifetimes were the main advantage. Lighting applications require LEDs with greatly improved efficiency that is typical for modern high-brightness LEDs.

The main physical reason that light extraction is difficult is the large ratio of the refractive indices of the semiconductor and the surrounding media. Consequently, a major part of the light generated inside a chip is reflected back into the semiconductor. High-brightness LED designs implement additional means for easy photon escape. In this chapter we review the LED photonics, which is the key issue for solid-state lighting technology. We start from basic considerations determining the design and performance of high-brightness LEDs (Section 5.1). Practical designs of conventional (planar rectangular) high-brightness LEDs are discussed in Section 5.2. Section 5.3 deals with supplementary classical-optics means of extracting light from semiconductors (i.e., outcouplers), which requires unconventional technology. Finally, recent achievements in light extraction, based on modification of the photon density of modes, are discussed in Section 5.4.

5.1. BASICS OF LIGHT EXTRACTION

5.1.1. Escape Cones

Photons emitted in the active layer of an LED escape into the surroundings after complex travel within the chip. These photons get lost at each stage of the journey via absorption in the substrate, semiconductor layers, contacts, and in the epoxy dome. Estimation of the extraction efficiency is highly involved and requires the use of statistical methods for photon gas (Joyce *et al.* 1974, Schnitzer *et al.* 1993a,b, Boroditsky and Yablonovitch 1997, Lee and Song 1999). Below, we present a simplified approach based on conventional geometrical considerations (Lee 1998a,b).

Consider a planar rectangular light-emitting structure grown on an absorbing substrate and encapsulated in an epoxy dome—an *absorbing-substrate* (AS) *LED*. The refractive indices of the layers in the semiconductor structure are usually very close and one can use a single average value n_s for these layers. The refractive index of the dome epoxy is n_e. The structure is depicted in Fig. 5.1.1, which also shows some relevant rays. The photons generated in a certain point of the active layer (where isotropic generation is assumed) may escape into the epoxy dome only for directions contained in a cone with an apex of $2\theta_c$. The *critical angle* θ_c is given by *Snell's law*

$$\theta_c(n_e, n_s) = \sin^{-1}\left(\frac{n_e}{n_s}\right). \tag{5.1.1}$$

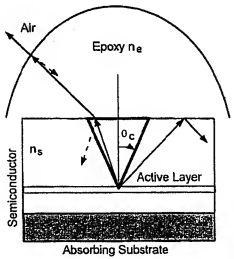

FIG. 5.1.1. Schematic of an escape cone in a conventional LED encapsulated in an epoxy dome.

Some of the light propagating within the *escape cone* is reflected from the semiconductor–epoxy interface. Additionally, some of the photons that escaped into the dome are reflected from the epoxy–air interface. The photons that are incident to the semiconductor surface with the angles $\theta > \theta_c$ propagate outside the escape cone and undergo the total internal reflection. In the structure shown in Fig. 5.1.1, most of the light which did not escape into the air on the first pass is lost due to absorption in the substrate and electrode area. This design, based on one escape cone, is typical of low-brightness LEDs with thin epitaxial structures grown on a light-absorbing substrate (Fig. 5.1.2a).

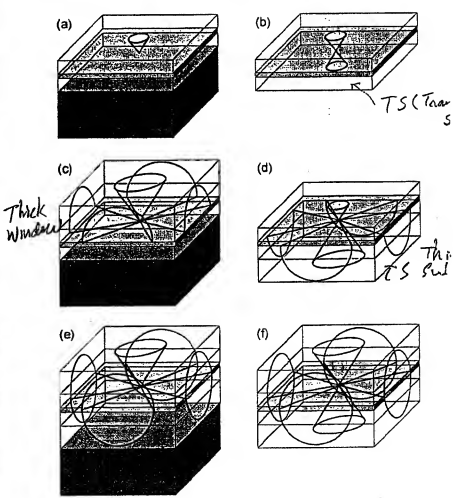

FIG. 5.1.2. LED designs with different numbers of escape cones.

One of the basic approaches employed in high-brightness LEDs is to increase the number of escape cones (Stringfellow and Craford 1997). In a rectangular configuration, up to six escape cones may be opened. A twofold improvement in extraction efficiency is achievec by removing the absorbing substrate or by introducing a transparent substrate (Ishiguro et al. 1983). Figure 5.1.2b shows the hypothetical design of a thin-structure two-cone *transparent-substrate* (TS) *LED* with an additional downward cone opened. Since the chip requires some thick support, the two-cone configuration might be imitated by introducing a mirror between the AS and the emitting structure (see Section 5.1.2 and Fig. 5.1.3).

Opening of the lateral cones is based on introduction of thick transparent layers on both sides of the electroluminescent structure. For instance, if the thickness of the upper transparent layer is increased, four lateral semicones emerge (Huang *et al.* 1992). For an appropriate thickness of the upper layer, often called the *window layer* (WL), the semicones are opened completely and three full cones are available for light escape. A three-cone WL LED schematic is shown in Fig. 5.1.2c. Similar thickening of the transparent substrate (Cook *et al.* 1988) adds four more semicones to the initial two-cone configuration, and the total number of escape cones becomes four (Fig. 5.1.2d). A five-cone design is available by growing both lower and upper WLs of sufficient thickness on an absorbing substrate (Fig. 5.1.2e). Finally, the most efficient six-cone design (Fig. 5.1.2f) is implemented by sandwiching the thin electroluminescent structure between two thick transparent layers, substrate and window (Kish *et al.* 1994a).

The extraction efficiency of an LED, in which an integer number of cones, N, is employed, is given by

$$\eta_{\text{opt}} = \frac{4n_e}{(n_e+1)^2} \times \frac{1-\sqrt{1-(n_e/n_s)^2}}{2} \times \sum_{j=1}^{N} T_i \,. \tag{5.1.2}$$

The first multiplier on the right-hand side of Eq. (5.1.2) accounts for the Fresnel reflection losses at the epoxy–air interface under the assumption that the photons reflected within the epoxy dome are not utilized. For a typical value of $n_e = 1.50$, this yields 0.96. The second multiplier is the fractional solid angle for a single escape cone $[(1-\cos\theta_c)/2]$. The third multiplier is the sum of the transmittances for each of the N cones ($0 \le T_i \le 1$) at the semiconductor–epoxy interface. Generally, some escape cones are partially shielded by the contacts that absorb the light. Also, the lateral cones may not be opened completely (truncated) because of insufficient layer thickness. However, when the bases of the opposite cones are separated by a low-optical-density structure, these two cones are coupled so that a photon reflected at the base of one of the cone might escape through the opposite cone (Lee 1998a).

Multiple reflections might lead to negligible Fresnel losses in a coupled cone pair since only an optically thin layer separates the escape surfaces. With the shielding neglected, transmittance of the completely opened cones is given by

$$T_i = \begin{cases} 1 & \text{for coupled opposite cones,} \\ 4n_s n_e/(n_s+n_e)^2 & \text{for uncoupled cones.} \end{cases} \tag{5.1.3}$$

Here the average reflectivity in the cone-base area is assumed equal to that for normal incidence. The cones next to the absorbing substrate and the opposite cones operating in the one-pass regime (i.e., with bases separated by an optically dense layer) must be treated as uncoupled cones.

In AlGaAs materials ($n_s \approx 3.5$), Eqs. (5.1.2) and (5.1.3) yield $\eta_{\text{opt}} \approx 0.04$ for a one-cone AS LED and $\eta_{\text{opt}} \approx 0.093$ for two coupled cones. For three pairs of uncoupled cones (six cones), $\eta_{\text{opt}} \approx 0.23$ for AlGaAs and $\eta_{\text{opt}} \approx 0.25$ for AlGaInP ($n_s \approx 3.4$), respectively.

The average refractive index of AlInGaN materials ($n_s \approx 2.5$) is smaller than that of AlGaAs and AlGaInP. Thus, even the primitive one-cone AS LED design yields $\eta_{\text{opt}} \approx 0.092$. In practical AlInGaN-based LEDs, the concept of escape cones is modified, since the semiconductor structure is placed on a transparent substrate with a refractive index n_i that satisfies the condition $n_e < n_i < n_s$ (Lee 1998b). In this case, the downward cone is enhanced. Additionally, a fraction of the photons that undergo total internal reflection from the top surface might escape through the transparent substrate (see Section 5.2.3).

5.1.2. Distributed Bragg Reflectors

The transparent substrate, which is one of the key elements in increasing the number of escape cones, is difficult to implement in some material/substrate systems. Fortunately, the downward escape cone can be replaced by an appropriate mirror positioned between the active layer and the absorbing substrate. An approach suitable for planar structures is the use of *distributed Bragg reflectors* (DBRs). A DBR structure consists of a number of alternating layers of high- and low-refractive-index materials (n_H and n_L, respectively) with an optical thickness of a quarter of the emission wavelength. The thickness of the layers is given by (Sugawara *et al.* 1993)

$$h_H = (\lambda_0/4)/(n_H \cos\theta_H), \tag{5.1.4a}$$

$$h_L = (\lambda_0/4)/(n_L \cos\theta_L), \tag{5.1.4b}$$

where λ_0 is the emission wavelength in air, and θ_H and θ_L are the incident angles at each individual layer. The higher the number of periods and the difference in refractive indices, the higher is the reflectivity of the DBR structure. A large

difference in the refractive indexes is also desirable for wide-band operation. The schematic design of a *DBR LED* is shown in Fig. 5.1.3. Kato *et al.* (1991) and Saka *et al.* (1993) were first to develop this approach for increasing the efficiency of infrared GaAs/AlGaAs LEDs grown on an absorbing GaAs substrate. Soon after, high-brightness AlGaInP LEDs in the orange-to-green color region were devised using DBR structures consisting of AlInP/AlGaInP layers (Sugawara *et al.* 1992a) or AlInP/GaAs (Itaya *et al.* 1994) layers (see Section 5.2.2). An AlGaAs red LED with an AlAs/AlGaAs DBR (Thomas *et al.* 1995) and an AlInGaN blue LED with a GaN/AlGaN DBR (Nakada *et al.* 2000) were also reported. Typically, 10- to 20-period DBRs are employed.

As can be seen from Eq. (5.1.4), a simple DBR is a resonant structure operating in a limited range of incident angles for a particular wavelength. This is ideal for laser diodes, but it does not always work well for LEDs, which isotronically emit a broad photon spectrum. To provide high reflectivity in a wide-angle, broad-spectrum regime, more sophisticated DBRs have been developed. A cascade of AlAs/AlGaAs quarter-wave reflector stacks designed for different wavelengths was demonstrated by Lee (1995). This design expanded the high-reflectance band in the red region. Combined (hybrid-type) DBR structures, consisting of different multilayers, were introduced for green AlGaInP LEDs. A typical hybrid DBR structure consists of two stacks of multilayers, either AlInP/AlGaInP or AlInP/GaAs (Sugawara *et al.* 1994b) or AlInP/AlGaInP and GaAs/AlAs (Chiou *et al.* 2000). Another way to attain a wide reflectance band is to utilize a chirped DBR structure, where the optical thickness of the alternating layers varies monotonically (Saka *et al.* 1993). A yellow-green AlGaInP LED with a chirped DBR structure was fabricated by Chang *et al.* (1997a).

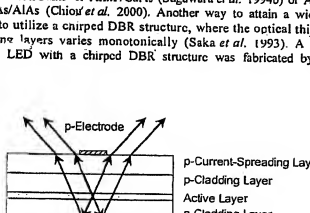

FIG. 5.1.3. Schematic design of a DBR LED.

5.1.3. Absorption Losses and Photon Recycling

The photons that do not escape through the cones are eventually absorbed in the chip. The irreversible (parasitic) losses are due to the absorption in the substrate and the contact area. Substrate losses are avoided by removing the substrate, using a transparent substrate, or redirecting the emission as described in Section 5.1.2.

Another important issue in the utilization of escape cones is to minimize parasitic absorption in the contact area. One possible solution is use of the aforementioned transparent electrodes (see Section 4.3.2). This idea is implemented in practical AlInGaN LEDs, where a thin Ni/Au ohmic metal is deposited on top of the chip (Nakamura *et al.* 1993d, 1994a, Lee 1998b; see also Section 5.2.3). Also, low optical absorption has been achieved by depositing indium-tin oxide (ITO) contacts on AlGaInP (Lin *et al.* 1994b, Aliyu *et al.* 1992) and GaN (Margalith *et al.* 1999) as well as indium oxide (In_2O_3) on AlGaAs (Thomas *et al.* 1995). An advantage of a transparent contact is that it also serves as a current-spreading layer (CSL). However, highly conductive transparent contacts might not be available or be difficult to implement in a particular materials system. In these cases, this problem has to be solved by other means. One possible solution is to avoid the light generation underneath the contact. A *current-blocking layer* (CBL) under the top electrode (Sugawara *et al.* 1992a; see Fig. 5.2.2a) or, in LEDs with a top ring contact, a *current aperture* (Windisch *et al.* 1998a) is introduced to implement this idea. Another way to reduce parasitic losses is to use electrode patterning (Ishiguro *et al.* 1983; see Figs. 5.2.1b and 5.2.2b).

However, in a well-designed LED, most of the losses are due to absorption in the active layer and, to some extent, in the surrounding transparent cladding and window layers. The losses in the active layer depend strongly on the probability of light reemission, since the photons absorbed can experience reincarnation and get a new chance to find the escape cone. If the internal quantum efficiency were high, the photon would be recycled many times until it escapes [the theory of photon recycling in LEDs is discussed by Baba *et al.* (1996) and in references therein]. Hence, light-extraction efficiency is a function of internal quantum efficiency, as shown by Boroditsky and Yablonovitch (1997). For instance, extremely high external quantum efficiency (72%) was demonstrated in an optically pumped AlGaAs/GaAs double heterostructure mounted on a high-reflectivity surface (Schnitzer *et al.* 1993a). Multiple photon recycling was due to internal quantum efficiency as high as 99.7%. A GaAs LED utilizing photon recycling with an external quantum efficiency of 12.5% was reported by Patkar *et al.* (1995). It should be noted that internal quantum efficiencies close to unity are needed in order to exploit the advantages of photon recycling. Therefore, the recycling technique is extremely sensitive to material quality and parasitic losses. A straightforward way to use photon recycling is the utilization of a thick active layer with a high internal quantum efficiency in order to catch and recycle as many nonescaped photons as possible. An example of this approach is a highly efficient AlGaAs/GaAs LED integrated with a quantum-well infrared detector (Dupont *et al.* 2000, Dupont and Chiu 2000). Nevertheless, in practical LEDs, the internal quantum efficiency is lower than 100% (and it decreases with aging) and the absorption in the active

layer is often considered as parasitic. Therefore, thin active layers (homogeneous or comprised of multiple wells) are often preferred. An optimum active-layer thickness involves a trade-off between active-layer reabsorption and electron confinement and depends on the emission wavelength (Gardner *et al.* 1999).

5.2. PHOTONICS OF PLANAR RECTANGULAR HIGH-BRIGHTNESS LEDs

The design of high-brightness LEDs is aimed at the high efficiency of light extraction and uses the escape-cone concept and low-parasitic-loss approaches (Stringfellow and Craford 1997). Cost pressures (Craford 1996) result in diverse schemes for commercial high-brightness LEDs utilizing different material systems. In this section we discuss the designs of practical AlGaAs, AlGaInP, and AlInGaN high-brightness LEDs that are manufactured using conventional planar rectangular technologies.

5.2.1. AlGaAs Red LEDs

Steranka (1997) described the photonics of practical AlGaAs LEDs. As we mentioned in Section 4.2.2, the main advantage of an AlGaAs/GaAs materials system is a very small lattice mismatch (lattice constants of GaAs and AlAs differ by less than 0.2% at 25°C). This makes feasible the growth of high-quality AlGaAs films on GaAs substrates. Thick and transparent layers (with high Al content) that are required for opening the lateral escape cones are easily produced using liquid-phase epitaxy (LPE) (Rupprecht *et al.* 1967).

Starting with the introduction of a thick window layer to improve light extraction in a single-heterostructure (SH) AlGaAs LED by Nishizawa *et al.* (1977), the quantum efficiency of the device was gradually increased (Varon *et al.* 1981, Nishizawa *et al.* 1983). Although an SH-AS version of the LED is still available, it exhibits moderate performance comparable to that of a red-filtered incandescent lamp. Implementation of a double heterostructure (DH) and transparent substrate by Ishiguro *et al.* (1983) and Cook *et al.* (1988) led to 21% external quantum efficiency (Ishimatsu and Okuno 1989). Since the internal quantum efficiency in AlGaAs is ~80% (Steranka *et al.* 1995), this value for the external quantum efficiency is close to the highest value obtainable in a six-cone design. Therefore, the design of AlGaAs red LEDs has undergone no significant improvements ever since.

Figure 5.2.1 shows two basic designs of commercial high-brightness AlGaAs LED chips with a DH active layer. The active layer is sandwiched between the wide-bandgap cladding layers. A version of a DH-AS LED is depicted in Fig. 5.2.1a. Figure 5.2.1b presents the design of a DH-TS LED. In the latter case, the GaAs substrate is removed by selective etching, and a patterned back contact is deposited.

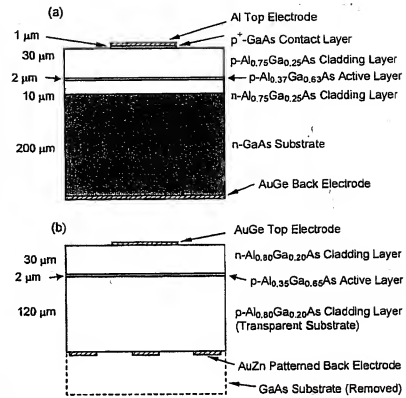

FIG. 5.2.1. Typical chip structures of high-brightness AlGaAs double-heterostructure LEDs: (a) absorbing substrate (DH-AS) LED; (b) transparent substrate (DH-TS) LED. (After Steranka 1997.)

The attainable thickness of the high-quality upper window layer is about 30 μm. This may be insufficient for complete opening of the upper lateral semicones. Other losses occur because of shielding of the vertical escape cones by the contacts. Photon absorption in the ohmic region, produced by metallization, is due mainly to the amorphous nature of the crystal in this region (Lee 1998a). The shielding extends over a significant area, since the top contact must be at least of 80 to 100 μm in diameter for high-speed wire bonding and the patterned back contact covers about 30% of the surface. With these losses taken into account, our estimate of the extraction efficiency in a TS LED for a typical chip width of 210 μm is about 19%, which is somehow lower than that observed. The actual light extraction efficiency is probably increased due to the randomization of photon trajectories at the chip walls formed by sawing (Schnitzer *et al.* 1993a, Lee 1998a).

luminescence intensity measured was up to 46 times higher than that of unprocessed wafers. Such a structure can be developed into an electroluminescent device with metal mirrors used as contacts.

5.4.3. Photonic Crystals

In structures with a periodically patterned refractive index, photons exhibit wave properties similar to that of electrons in crystals. Called *photonic crystals*, such structures can be implemented in one, two, or three dimensions (see Fig. 5.4.3). Similar to what is done for electron waves in conventional crystals, the propagation of electromagnetic waves in photonic crystals is described by concepts of reciprocal space, Brillouin zones, dispersion relations, Bloch wavefunctions, Van Hove singularities, and effective masses (Yablonovitch 1993, Joannopoulos *et al.* 1995).

In a photonic crystal, photon modes disappear for particular (forbidden) frequencies and directions, while the density of modes can increase for other (allowed) frequencies and directions (John 1987, Yablonovitch 1987). As a result, spontaneous emission can be either inhibited or enhanced (Yablonovitch *et al.* 1988). A defect introduced into a photonic crystal produces a localized state within the bandgap (Yablonovitch *et al.* 1991b). This means that natural spontaneous emission can be supported only in one favorable mode and suppressed in other modes. Actually, a DBR–DBR RC LED (Fig. 5.4.1b) implements the concept of a one-dimensional photonic crystal with a defect (λ or $\lambda/2$ cavity) included. However, in this LED, the advantages of photonic crystal are poorly exploited because only a single dimension is used.

Two-dimensional (2D) photonic crystals (Plihal *et al.* 1991, Plihal and Maradudin 1991) offer more possibilities for photon density-of-states engineering. Commonly, the structures consist of periodic arrays of parallel cylindrical rods (e.g., semiconductor pillars in air or cylindrical holes in a layer; Villeneuve and Piché 1992) as shown in Fig. 5.4.4. Large photonic bandgaps for all lateral directions and for any polarization are obtained in arrays of triangular (hexagonal; Meade *et al.* 1992) and honeycomb (graphite; Cassagne *et al.* 1996) symmetry provided that the refractive index contrast is high. A variety of techniques for fabrication of 2D photonic crystals already exist (lithography and etching, electrochemistry, vertical selective oxidation, epitaxial lift-off, etc.; see the review paper by Krauss and De La Rue 1999). Semiconductor-based 2D photonic crystals with the bandgap in the near-IR range were demonstrated in GaAs/AlGaAs (Gourley *et al.* 1994, Krauss *et al.* 1994) and InGaAs/InP (Baba and Koma 1995, Baba and Matsuzaki 1996) materials systems. In the visible, a 2D photonic bandgap was observed in nanochannel-glass structures (Lin *et al.* 1996).

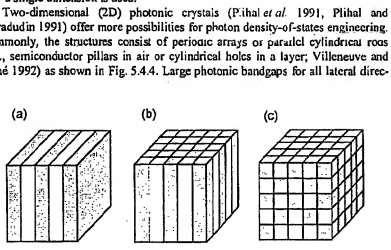

FIG. 5.4.3. Simple examples of photonic crystals: (a) periodic in one direction; (b) periodic in two directions; (c) periodic in three directions. Gray and white colors represent materials with different refractive indices. (After Joannopoulos *et al.* 1995.)

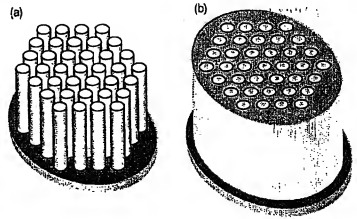

FIG. 5.4.4. Typical structure of 2D photonic crystals: (a) periodic array of semiconductor pillars; (b) air rods in a semiconductor layer.

Light extraction from a thin slab of 2D photonic crystal was considered by Fan *et al.* (1997a). The extraction efficiency was predicted to exceed 90% due to the elimination of guided modes. A schematic design of the proposed light-emitting device that exploits a 2D photonic crystal (Baba 1997, Fan *et al.* 1997b) is shown in Fig. 5.4.5. The chip features a semiconductor slab, which contains an active layer sandwiched between cladding layers. To inhibit lateral emission, a triangular lattice of air holes is patterned into the slab. The slab may be placed over a DBR structure that directs emission only through the top surface. Enhancement and suppression of spontaneous emission in a thin-film InGaAs/InP photonic crystal was demonstrated by varying the period of the hexagonally arrayed holes (Boroditsky *et al.* 1999b). Similarly, the device may be composed of an array of dielectric rods in air. Baba *et al.* (1999) demonstrated the latter version of a 2D-photonic-crystal emitter by fabricating a honeycomb array of InGaAsP/InP micropillars. The emitter exhibited a more than tenfold increase in photoluminescence extraction compared with a planar wafer.

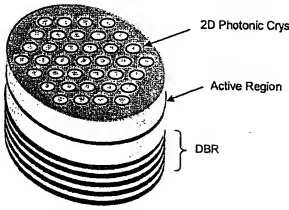

FIG. 5.4.5. Outline of a semiconductor light-emitting device comprising a 2D photonic crystal and a DBR structure. (After Baba 1997 and Fan *et al.* 1997b.)

One of the limiting factors for these nanometer-scaled devices is surface recombination, since patterning of the semiconductor layers (such as shown in Fig. 5.4.4) results in considerable enhancement of the surface-to-volume ratio. Boroditsky *et al.* (2000) investigated the surface recombination velocity in III–V candidate materials for nanostructure LEDs. A gallium nitride system and chemically passivated InGaAs were shown to possess relatively low surface recombination velocity ($\sim 10^4$ cm/s), while an AlGaInP materials system exhibited a value that is an order of magnitude higher.

Boroditsky *et al.* (1999a,b) reported on a promising thin-slab LED design which uses highly efficient external scattering of light by a 2D photonic crystal. The light was generated in an unpatterned InGaAs/InP heterostructure of 20-μm width. The generation region was surrounded by a photonic crystal, which was a thin film patterned by a hexagonal array of air holes. The photonic structure did not influence spontaneous emission but improved light extraction via coherent scattering of internally trapped light. The device exhibited photoluminescence yield with 70% quantum efficiency. Ochoa *et al.* (2000) proposed a similar structure surrounded by circular concentric deep-etched trenches that acted as a 2D Bragg mirror. A sixfold enhancement in light extraction of an InGaP/InGaAs LED was achieved by using a 2D photonic crystal inside the upper cladding layer (Erchak *et al.* 2001).

Fabrication of 3D photonic crystals with a lattice constant in the optical range is being developed. For example, a face-centered-cubic photonic structure can be produced by etching three sets of holes 35.26° off the vertical direction into the semiconductor surface (Yablonovitch *et al.* 1991a). GaAs structures with a photonic bandgap in the near IR were fabricated in such a way by applying chemically assisted ion-beam etching of the masked surface in three directions (Cheng *et al.* 1996, 1997). Another fabrication method relies on stacking selectively etched 2D structures by wafer bonding. Using this method, 3D stacks of GaAs (Noda *et al.* 1996, Yamamoto *et al.* 1998) and InP (Noda *et al.* 1999) rods were produced. A different technique of stacking semiconductor rods into a 3D photonic crystal was proposed (Lin *et al.* 1998, Fleming and Lin 1999). The stack of Si rods was produced by repetitive deposition, patterning, and etching trenches in SiO_2 layers and filling of the trenches with polysilicon. This technique allowed fabrication of an IR 3D photonic crystal with single-mode defect cavities (Lin *et al.* 1999).

The availability of 3D photonic crystals for operating in the visible spectral range still suffers from a lack of workable technologies. At present, the only implementation of a 3D photonic bandgap in the visible range is based on utilization of self-organized systems (John and Busch 1999). For example, Astratov *et al.* (1996) used synthetic opals composed of silica (α-SiO_2) spheres closely packed in a face-centered-cubic structure with a period of about 200 nm. By filling the voids between the spheres with a semiconductor with a refractive index higher than that of silica, photonic bandgaps for some directions (pseudogaps) might be realized. 3D photonic crystals formed of opal filled with CdS (Astratov *et al.* 1996, Vlasov *et al.* 1997a) and InP (Romanov *et al.* 1997) were demonstrated. Both enhancement (Vlasov *et al.* 1997b) and inhibition (Blanco *et al.* 1998) of optical emission in CdS quantum dots embedded inside the interstitials between the silica spheres were achieved.

All in all, photonic crystals remain an intriguing idea for future light emitters with external quantum efficiencies close to unity. However, a lot of effort will be required to make this idea feasible for solid-state lighting applications.